In important, also, for the polarity of the electrodes, the ferrite changes polarity (−) to ferrite (+), thus, different results are obtained, as shown in the figure, this determines that the use of ferrite with the polarity (−) is the best option. The diffraction efficiency obtained with ferrite electrodes (−) and copper (+) was 5.2%, approximately, with the copper electrodes was of the order of 3.6%, with ferrite electrodes (+), copper (−) was 3.5% approximately, and without voltage was 3.4%.

Figure 17, is very interesting because it clearly shows a big difference when 30 V is applied to the electrodes of ferrite (−) and copper (+), and without voltage. Another interesting point is the polarity of the electrodes of copper, when changed from (+) to (−), one would expect it to be the same, but the nature of materials reserve some surprises, as shown in this graph. It suggests that the material preferably has a polarity determined by the salts comprising the photosensitive emulsion. The diffraction efficiency obtained with ferrite electrodes (−) and copper (+) was approximately 3.3%, with the copper (+) and copper (−) was of the order of 0.6%, with copper (−) and copper (+) was approximately 0.8%, and without voltage was 0.4%, although all measurements are within the error range, which corresponds to 0.5% in diffraction efficiency. Figures 15–17 did not introduce the range of error in the graphs for the to reader have more clarity of the information.

Figure 17. Diffraction efficiency of 30 V voltage with thickness of 52 µm of sample F with a frequency of 1132 lines/mm, using different electrodes.

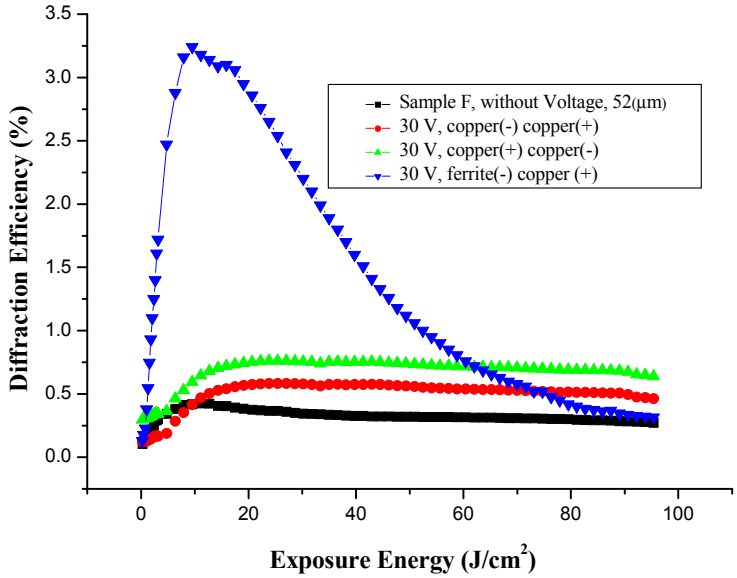

3.5.4. Microstructure of Gratings

The images of gratings with sample C were obtained with an Olympus BX51 Optical Microscope®, (Hicksville, NY, USA). The image (a) corresponds to a photomicrograph of the grating without voltage, clearly being observed from grooves forming in the grating. The red background is the filter used with the microscope. Image (b) is a photomicrograph of the grating with 30 V, with more diffraction efficiency, by a factor of 1.3 times, with respect to the grating (a).

The increase in diffraction efficiency is determined by the factors described in Section 3.6, by the process of crosslinking of iron with the photochemical reaction of the reduction of Fe^{3+} to Fe^{2+} ion, and condensation of water, see Figure 18b.

Figure 18. Photomicrograph of diffraction gratings with 454 lines/mm, sample C, (**a**) without voltage, (**b**) with voltage.

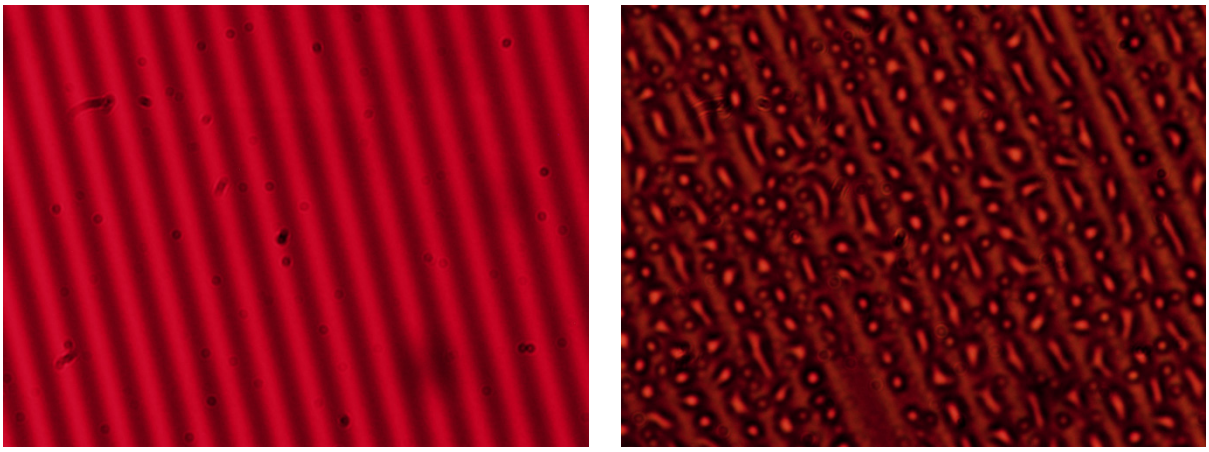

(**a**) (**b**)

An important point of the gratings, with 30 V, is the accumulation of micro-droplets (condensation of water) on microgrooves of orderly form. This contributes to increase the diffraction efficiency. The microdroplets on the grooves generate a small scattering on the diffracted orders, due to the shape and size variation of the microdroplets. This phenomenon is repeated for all frequencies from 454 to 1132 lines/mm, and for concentrations C and F.

3.6. Discussion

The hypothesis describes process of photo-crosslinking through electron transfer with formation and mobility of ion-radical active and non-active in system. With reorientation of electric charges and polarity between atoms and molecules the intramolecular crosslinks are formed in the hologram. This process is essentially through electron transfer from photochemical reduction reaction of Fe^{3+} to Fe^{2+} ion. Finally, electrochemical voltaic interaction contributes to a photo-redox process, increasing more the diffraction efficiency, and changing absorption in the film, taking a dark appearance.

An interesting result of Figure 18b is the condensation of water, which plays an important role in increasing the diffraction efficiency of gratings. This physical phenomenon is external to the electrochemical processes in the hypothesis posed. These are complementary phenomena.

3.6.1. Hypothesis Mechanism for Holographic Recording and Voltage Effect

The process describes possible chemical reactions for the preparation of PVA-$FeCl_3$ hologram. Starting with preparation of the aqueous solution of polyvinyl alcohol (PVAaq) 7% and 80 °C, Equation (3) [37–46]. The aqueous solution of ferric chloride, $FeCl_{3(aq)}$, Equation (6) to 10% at 25°C, water ionization described in hydrogen ions (H^+) and hydroxide ions (OH^-), Equation (4). These, interact with ferric chloride crystals generating the solution of ferric ions (Fe^{3+}) and chloride ions (Cl^-), resulting a solution of ferric chloride with acidic properties, Equation (5). The reactions of ions (Fe^{3+} + $3OH^-$) produce ferric hydroxide, $Fe(OH)_3$. With removal of OH^- (hydroxyl) ions in aqueous solution causes a relative excess of hydrogen ions, H^+, which makes an acid solution [47–57]. Equation (7) shows the preparation of polymer matrix with an oxidizing agent. $PVA_{(aq)}$ and $FeCl_{3(aq)}$

are combined in a ratio 10:2 and 10:5, at 25 °C, with conventional drying of samples C and F for 24 h at normal laboratory conditions. Starting here, the intramolecular interaction of components [18,19]: a film of yellow light brown [PVA:$FeCl_3$]·xH_2O is generated. The image (grating) is recorded, through of photo-crosslinking process with the photo-activity of ferric ions (Fe^{3+}) with chloride ions (Cl^-) and hydroxide ions (OH^-) in acidic medium. Thus, Equations (8) and (9) represent the formation of photo-active intermediate species that coexist with [Fe^{3+}·Cl^-] and [$Fe^{3+}OH^-$], to pH = 2. With a photon absorption of λ = 445 nm, the process continues until reaching photo-reduction of iron with generation of ferrous ions (Fe^{2+}) and free radicals, both chlorine (Cl) and hydroxyl (OH). With the process of photo-crosslinking there is the formation of three types of Fe, active and inactive Fe^{3+}, and Fe^{2+} inactive [56–67]. Equation (10) represents the polymer matrix, [PVA:$FeCl_3$]·xH_2O, exposed to laser λ = 445 nm, a state transition is produced, [$Fe^{3+}Cl^-$---PVA---$Fe^{3+}OH^-$] + H^+, by electronic excitation, where main photo-active species interact with PVA and generate hydrogen radical-cation. The species [$Fe^{3+}OH^-$] is more active, and photo-chemically less active, known as iron (III) aqueous, $Fe^{3+}_{(aq)}$, [18,19]. The photo-redox process continues for transfer of electrical charges being obtained the photo-crosslinked (recorded image), [PVA-OH-Fe^{2+}], with the production of ferrous chloride ($FeCl_2$), ferrous hydroxide, $Fe(OH)_2$, ferric hydroxide, $Fe(OH)_3$, hydrogen gas, H_2, and chlorine gas, Cl_2, [53,68–75] this process darkens the sample film. Lastly, the photo-electrochemical process is performed by a redox reaction. Equation (11) represents chemical reaction simulation, where film is recorded simultaneously with voltage application [76–78]. The photo-crosslinking process [PVA-OH-Fe^{2+}] with humidity and 30 V, with copper electrode (anode) and ferrite electrode (cathode), separated by 5 mm. The electric field contributes to increase diffraction efficiency of the holographic grating recording process [PVA-OH-Fe^{2+}]*****. Substances obtained: hydroxides of Fe (II) and Fe (III), chlorides of Cu (II) and Fe (II), and H_2 and Cl_2 gas, [69–71]. By the electronegativity the copper, Cu, replaces the iron atom, Fe, in the system. Apart of the photochemical and electrochemical processes, we note that when the applied electric field the holographic grating recording. It produces a condensation of water located on the grooves of the gratings.

3.6.2. Diagram Chemical Reactions

Preparation of PVA-$FeCl_3$ for holographic recording.

PVA aqueous solution:

$$PVA_{(s)} + H_2O_{(l)} \xrightarrow[7\%_{(l)}]{T=80\ ^\circ C} PVA_{aq} \quad (3)$$

aq = solute disolved in water; s = solid; l = liquid; ↑ = gas.

Ionization of H_2O and $FeCl_3$:

$$H_2O_{(l)} \rightleftharpoons H^+ + OH^- \quad (4)$$

$$FeCl_3 \xrightarrow{H^+/OH^-} Fe^{3+}_{(aq)} + 3Cl^-_{(aq)} \quad (5)$$

Acid solution of ferric chloride:

$$FeCl_{3(s)} + H_2O_{(l)} \xrightarrow[10\%]{T=25^\circ C} FeCl_{3(aq)} \quad (6)$$

Polymer matrix with oxidizing agent:

$$PVA_{(aq)} + FeCl_{3(aq)} \xrightarrow[10:2/24h]{T=25^{\circ}C} [PVA\!:\!Fe_3Cl_3]\bullet\times H_2O\,(\text{brown dry film}) \quad (7)$$

Photo-active of Fe^{3+} ions in acidic medium for holographic recording:

$$Fe^{3+} + Cl^{\bullet -} \xrightarrow[(H^+/OH^{-})]{h\nu=445nm} \underset{(\text{photoactive species})}{[Fe^{3+}\bullet Cl^-]} \xrightarrow[\text{photo-reduction}]{h\nu=445nm} [Fe^{2+} +^{\bullet} Cl] \quad (8)$$

$$Fe^{3+} + OH^{\bullet -} \xrightarrow[(H^+/OH^{-})]{h\nu=445} \underset{(\text{photoactive species})}{[Fe^{3+}\bullet OH^-]} \xrightarrow[\text{photo reduction}]{h\nu=445nm} [Fe^{2+} +^{\bullet} OH] \quad (9)$$

Photo-crosslinking in the film, image recording:

$$\begin{aligned} &[PVA\!:\!FeCl_3]\bullet\times H_2O \xrightarrow{h\nu=445nm} \underset{\textit{Transition state}}{[Fe^{3+}\bullet Cl^- \text{---PVA---} Fe^{3+}\bullet OH^-]} + \bullet H^+ \\ &\xrightarrow{h\nu=445nm} \underset{\text{photo-crosslinked (image)}}{[PVA\text{-}OH\text{-}Fe^{2+}]} + FeCl_2 + Fe(OH)_2 + Fe(OH)_3 + H_2\uparrow + Cl_2\uparrow \end{aligned} \quad (10)$$

Over all reaction, preparation of the holographic grating with voltage application:

$$\begin{aligned} &[PVA\text{-}OH\text{-}Fe^{2+}] + H_2O_{\text{moisture}} + FeCl_{3(aq)} + \underset{\text{active}}{Fe(OH)_3} + \underset{\text{anode}}{Cu_{(s)}} + \underset{\text{cathode}}{Ferrite_{(s)}} \\ &\xrightarrow[30\,V]{h\nu=445nm} \underset{\substack{\text{photo-crosslinked}\\(\text{image with Voltage})}}{[PVA\text{-}OH\text{-}Fe^{2+}]^*} + \underset{\text{Inactive}}{Fe(OH)_3} + Cl_2\uparrow + H_2\uparrow + FeCl_2 + CuCl_2 + Fe(OH)_2 \end{aligned} \quad (11)$$

Figure 19, presents a 2D schematic of the vicinity of the copper electrode (anode) and ferrite (cathode) by applying a voltage of 30 V, showing the electrochemical redox process, based in the explaining of the Equation (11).

Figure 19. Scheme 2D, simplified representation of the electrochemical interactions as from photo-redox process the grating (image) [PVA-OH-Fe^{2+}]*****. The formation of the image (grating) without voltage is: [PVA-OH-Fe^{2+}], when voltage is applied is: [PVA-OH-Fe^{2+}]*****. This * is, to differentiate both images.

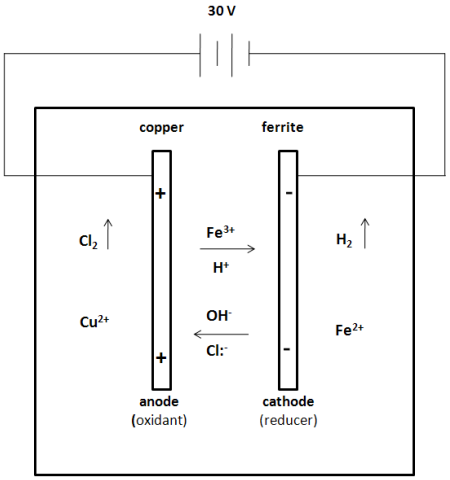

4. Conclusions

Holograms formed with PVA and $FeCl_3$ have two components, phase and amplitude. Generally we know that the phase contributes more significantly to the diffraction efficiency than the amplitude. PVA is a hydrophilic material; the prepared emulsion always has a humidity component that promotes the electrical conduction of the material and gratings recording. If the sample is completely dry, without wetness, the material is not photosensitive. We investigated the diffraction efficiency of holographic gratings made with different concentrations of $FeCl_3$ dopant. We describe the sample preparation and report the chemical characteristics of the solutions with respect to the $FeCl_3$ concentration. The experimental results show, as well, the diffraction efficiency with respect to the chemical and physical characteristics of samples, exposure energy, and registration angle of the gratings. The diffraction efficiency of the samples under a voltage applied to the hologram was obtained. We experimentally observed that the dopant concentration affects the characteristics of the samples as: resistivity, pH, and absorbance. The principal chemical mechanism in the samples under an applied DC voltage is the oxide-reduction reaction and photocrosslinking of PVA bonds with the incident energy in holographic recording. The hypothesis on the formation of the grating and the effect of the applied voltage is shown. The values of some important parameters for holographic gratings can be changed in this material by varying the applied voltage. The phenomena involved here are complex as two interrelated behaviors are significant for holographic gratings recorded with and without an applied voltage, an increase in the diffraction efficiency by a factor of 1.3 times for sample C and 2 times for F when the voltage is applied, and a shift in the diffraction efficiency with time, these results are valid for low and high frequencies. An important point of the gratings with 30 V is the increase in diffraction efficiency that is determined by the factors described in Section 3.6, by the process of crosslinking of iron with the photochemical reaction of the reduction of Fe^{3+} to Fe^{2+} ion; forming the [PVA-OH-Fe^{2+}]***** image, together with condensation of water.

The condensation of water on microgrooves, contributes to an increase the diffraction efficiency and generate a small scattering on the diffracted orders, due to the shape and size variation of the microdroplets.

This phenomenon is repeated for all frequencies and concentrations.

These are preliminary results; in the future, the material will be characterized in greater depth to determine its nature and whether it is appropriate for use as a photorefractive material. Finally, the principal goal in this work is to use the metallic halides, which offer a good opportunity for obtaining photoconductive materials using metallic salts and these are inexpensive and easy to manipulate under room conditions.

Acknowledgments

Thank Institute National of Astrophysics Optical y Electronic (INAOE) for the support infrastructure and economic support.

Author Contributions

Arturo Olivares Pérez, directs, coordinates and funds the entire investigation. Mary Paz Hernández-Garay, cooperates in the investigation of the behavior of diffraction gratings with $FeCl_3$ and applied voltage.

Santa Toxqui-López, collaborated on the investigation of the behavior of diffraction gratings with $FeCl_3$ for different electrodes and gratings with high frequency. Israel Fuentes-Tapia, assists in the preparation of photosensitive films for different concentrations and performed the experimental setup. Manuel Jorge Ordóñez-Padilla, assists in the analysis and discussion of the photoreduction and photochemical processes involved in the formation of the image.

Conflicts of Interest

The authors declare no conflict of interest.

References

1. John, B.M.; Joseph, R.; Sreekumar, K.; Sudha-Kartha, C. Copper doped methylene blue sensitized poly(vinyl alcohol)-acrylamide films for stable diffraction efficiency. *Jpn. J. Appl. Phys.* **2006**, *45*, 8686–8690.
2. Pramitha, V. A New Metal Ion Doped Panchromatic Photopolymer for Holographic Applications. Ph.D. Thesis, Cochin University of Science and Technology: Cochin, India, November 2011.
3. Pramitha,V.; Nimmi, K.P.; Subramanyan, N.V.; Joseph, R.; Sreekumar, K.; Sudha Kartha, C. Silver-doped photopolymer media for holographic recording. *Appl. Opt.* **2009**, *48*, 2255–2261.
4. Solymar, L.; Cooke, D.J. *Volume Holography and Volume Gratings*; Academic Press: London, UK, 1981.
5. Finch, A. *Polyvinyl Alcohol Developments*; John Wiley and Sons: New York, NY, USA, 1992.
6. Nachtrieb, N.H. Conduction in fused salts and salt-metal solutions. *Ann. Rev. Phys. Chem*. **1980**, *31*, 131–156.
7. Patachia, S.; Rinja, M.; Isac, L. Some methods for doping poly (vinyl alcohol) hydrogels [PVA-HG]. *Rom. J. Phys*. **2006**, *51*, 253–262.
8. Gaafar, S.A.; Abd El-Kader, F.H.; Rizk, M.S. Changes in the structure of poly (vinyl alcohol)-CrCI composites irradiated by low level fast neutron doses. *Phys. Scr*. **1994**, *49*, 366–370.
9. MacDiarmid, A.G. Nobel Lecture: Synthetic metals: A novel role for organic polymers. *Rev. Mod. Phys.* **2001**, *73*, 701–712.
10. Valsangiacom, M.S.; Bulinski, M.; Iova, I.; Schinteie, G.; Kuncser, C.; Filoti G.; Bejan, D. Optical and electronic proprieties of mixed Fe-Sn doped PVA. *Rom. Rep. Phys*. **2003**, *55*, 283–286.
11. Sakhno, O.V.; Goldenberg, L.M.; Stumpe, J.; Smirnova, T.N. Surface modified ZrO_2 and TiO_2 nanoparticles embedded in organic photopolymers for highly effective and UV-stable volume holograms. *Nanotechnology* **2007**, *18*, doi:10.1088/0957-4484/18/10/105704.
12. Jamil, M.; Ahmad, F.; Rhee, J.T.; Jeon, Y.J. Nanoparticle-doped polymer-dispersed liquid crystal display. *Curr. Sci.* **2011**, *101*, 1544–1552.
13. Juhl, A.T.; Busbee, J.D.; Koval, J.J.; Natarajan, L.V.; Tondiglia, V.P.; Vaia, R.A.; Bunning, T.J.; Braun, P.V. Holographically directed assembly of polymer nanocomposites. *Acsnano* **2010**, *4*, 5953–5961.
14. Ostrowski, A.M.; Naydenova, I.; Toal, V. Light-induced redistribution of Si-MFI zeolite nanoparticles in acrylamide-based photopolymer holographic gratings. *J. Opt. A Pure Appl. Opt.* **2009**, *11*, doi:10.1088/1464-4258/11/3/034004.

15. Liu, X. Photopolymerizable Metal Nanoparticle-/Semiconductor Quantum Dot-Polymer Nanocomposite Materials for Nonlinear Optics. Ph.D. Thesis, The University of Electro-Communications Tokyo: Tokyo, Japan, March 2012.
16. Yovcheva, T.; Naydenova, I.; Sainov, S.; Toal, V.; Mintova, S. Holographic recording in corona charged acrylamide-based MFI-zeolite photopolymer. *J. Nonlinear Opt. Phys. Mater.* **2011**, *20*, 271–279.
17. Li, C.; Cao, L.; Yi, Y.; He, Q.; Jin, G. Plasmon-active mixed gratings in volume holographic polymeric nanocomposites. In Proceedings of Photonic Fiber and Crystal Devices: Advances in Materials and Innovations in Device Applications VII, San Diego, CA, USA, 25 August 2013.
18. Budkevich, B.A.; Polikanin, A.M.; Pilipovich, V.A.; Petrochenko, N.Ya. Amplitude-phase hologram recording on $FeCl_3$–PVA films. *J. Appl. Spectrosc.* **1989**, *50*, 621–624.
19. Manivannan, G.; Changkakoti, R.; Lessard, R.A. Cr (VI)- and Fe (III)-doped polymer systems as real-time holographic recording materials. *Opt. Eng.* **1993**, *32*, 671–675.
20. Bulinski, M.; Kuncser, V.; Plapcianu, C.; Krautwald, S.; Franke, H.; Rotaru, P.; Filoti, G. Optical and electric properties of polyvinyl alcohol doped with pairs of mixed valence metal ions. *Rom. Rep. Phys.* **2003**, *5*, 283–286.
21. Olivares-Pérez, A.; Hernández-Garay, M.P.; Fuentes-Tapia, I.; Ibarra-Torres, J.C. Holograms in polyvinyl alcohol photosensitized with $CuCl_2$ ($2H_2O$). *Opt. Eng.* **2011**, *50*, 065801:1–065801:6.
22. Hernández-Garay, M.P.; Olivares-Pérez, A.; Fuentes-Tapia, I. Characterization and evolution of electro-optical properties from holograms replication on polymer (PVA) with salts ($FeCl_3$). In Proceedings of 5th International Workshop on Information Optics (WIO'06), Toledo, Spain, 5–7 June 2006; pp. 446–454.
23. Skoog, D.A.; West, D.M.; Holler F.J.; Crouch, S.R. *Fundamentals of Analytical Chemistry*; Thomson-Brooks/Cole: London, UK, 2004; pp. 500–560.
24. Basolo, F.; Johnson, R. *Química de los Compuestos de Coordinación*; Reverté: Barcelona, Spain, 1978; pp. 81–100. (in Spanish)
25. Hamzah, H.M.; Saion, E.; Kassim, A.; Yousuf Hussain, M.; Shahrim Mustafa, I.; Ahmad Ali Omer, M. Temperature dependence of AC electrical conductivity of PVA-PPy-$FeCl_3$ composite polymer films. *Malays. Polym. J.* **2008**, *3*, 24–31.
26. Van Renesse, R.L. Photopolymers in holography. *Opt. Laser Technol.* **1972**, *4*, 24–27.
27. De Sio, L.; Veltri, A.; Tedesco, A.; Caputo, R.; Umeton, C.; Sukhov, A.V. Characterization of an active control system for holographic setup stabilization. *Appl. Opt.* **2008**, *47*, 1363–1367.
28. Frejlich, J.; Cescato, L.; Mendes, G.F. Analysis of an active stabilization system for a holographic setup. *Appl. Opt.* **1988**, *27*, 10, 1967–1976.
29. American Society for Testing and Materials. *Standard Test Methods for D-C Resistance or Conductance of Moderately Conductive Materials*; ASTM D4496-04; American Society for Testing and Materials: West Conshohocken, PA, USA, 2008.
30. Hariharan, P. *Basics of Holography*; Cambridge University Press: London, UK, 2002; pp. 15–24.
31. Kogelnik, H. Coupled wave theory for thick hologram gratings. *Bell Syst. Tech. J.* **1969**, *48*, 2909–2947.
32. Tawansi, A.; El-Khodary, A.; Abdelnaby, M.M. A study of the physical properties of $FeCl_3$ filled PVA. *Curr. Appl. Phys.* **2005**, *5*, 572–578.

33. Fontanilla-Urdaneta, R.C.; Olivares-Pérez, A.; Fuentes-Tapia, I.; Ríos-Velasco, M.A. Analysis of voltage effect on holographic gratings by modulation transfer function. *Appl. Opt*. **2011**, *50*, 1827–1831.
34. Korneev, N.; Flores Ramirez, O.; Bertram, R.P.; Benter, N.; Soergel, E.; Buse, K.; Hagen, R.; Kostromine, S.G. Pyroelectric properties of electrically poled photoaddressable polymers. *J. Appl. Phys*. **2002**, *92*, 1500–1503.
35. Kyritsis, A.; Pissis, P.; Gómez, R.J.L.; Monleón, P.M. Dielectric relaxation spectroscopy in PHEA hydrogels. *J. Non Cryst. Solids* **1994**, *2*, 1041–1046.
36. Ricciardi, R.; Auriemma, F.; de Rosa, C.; Lauprêtre, F. X ray diffacction analysis of poly(vinyl alcohol) hydrogels, obtained by freezing and thawing techniques. *Macromolecules* **2004**, *37*, 1921–1927.
37. Willcox, P.J. Microesturcture of poly(vinyl alcohol) hydrogels produced by freeze/thaw cycling. *J. Polym. Sci. Part B Polym. Phys.* **1999**, *37*, 3438–3454.
38. Valentín, J.L.; López, D.; Hernández, R.; Mijangos, C.; Saalwächter, K. Structure of poly(vinyl alcohol) cryo-hydrogels as studied by proton low-field NMR spectroscopy. *Macromolecules* **2009**, *42*, 263–272.
39. Hassan, C.M.; Peppas, N. Structure and morphology of freeze/thawed PVA hydrogels. *Macromlecules* **2000**, *33*, 2472–2479.
40. Mishra, R.; Rao, K.J. Electrical conductivity studies of poly (ethylene oxide) poly (vinylalcohol) blends. *Solid State Ionics*. **1998**, *106*, 113–127.
41. Awadhia, A.; Patel, S.K.; Agrawal, S.L. Dielectric investigation in PVA based gel electrolytes. *Prog. Cryst. Growth Charact. Mater*. **2006**, *52*, 61–68.
42. Trieu, H.H.; Qutubuddin, S. Polyvinyl alcohol hydrogels I. Microscopic structure by freeze-etching and critical point drying technique. *Colloid Polym. Sci*. **1994**, *272*, 301–309.
43. Singh, K.P.; Gupta, P.N. Study of dielectric relaxation in polymer electrolytes. *Eur. Polym. J.* **1998**, *34*, 1023–1029.
44. Londoño, M.E.; Jaramillo, J.M. Dielectric behavior of poly(vinyl alcohol) hydrogels preparing by freezing/thawing technique. *Revista EIA* **2011**, *165*, 132–137.
45. The Chemistry of Ferric Chloride. Available online: http://www.artmondo.net/printworks/articles/ferric.htm (accessed on 7 March 2014).
46. Sherman, D.M. Electronic structures of Fe^{3+} coordination sites in iron oxides: Applications to spectra, bonding and magnetism. *Phys. Chem. Miner.* **1985**, *12*, 161–175.
47. Sherman, D.M. Molecular orbital (SCF-X-SW) theory of Fe^{2+}-Mn^{3+}, Mn^{2+}-Fe^{3+} and Fe^{3+}-Mn^{3+} charge transfer and magnetic exchange interactions in oxides and silicates. *Am. Mineral.* **1990**, *75*, 256–261.
48. Sherman, D.M.; Waite, T.D. Electronic spectra of Fe^{3+} oxides and oxide hydroxides in the near-IR to near-UV. *Am. Mineral.* **1985**, *70*, 1262–1269.
49. Hudson, R.J.; Covault, D.T.; Morel, F.M. Investigations of iron coordination and redox reactions in seawater using ^{59}Fe radiometry and ion-pair solvent extraction of amphiphilic iron complexes. *Mar. Chem*. **1992**, *38*, 209–235.
50. Richards, D.H.; Sykes, K.W. Ionic association and reaction rates. Part I. A spectrophotometric study of the hydrolysis of iron (III). *J. Chem. Soc*. **1960**, *1960*, 3626–3633.

51. Balt, S.; Verwey, A.M.A. Electronicspectra and ligandfieldparameters in chloroaquoiron (III) complexes. *Spectrochim. Mol. Spectrosc.* **1967**, *23*, 2069–2075.
52. Heistand, R.N.; Clearfield, A. The effect of specific swamping electrolyte supon the formation constant of the monochloro iron (III) complex. *J. Am. Chem. Soc*. **1963**, *85*, 2566–2570.
53. Knight, R.J.; Sylva, R.N. Spectrophotometric investigation of iron (III) hydrolysis in light and heavy water at 25 °C. *J. lnorg. Nucl. Chem*. **1975**, *37*, 779–783.
54. Silverman, J.; Dodson, R.W. The exchange reaction between the two oxidation states of iron in acid solution. *J. Phys. Chem.* **1952**, *56*, 846–852.
55. Schugar, H.J. The structure of iron (III) in aqueous solution. *J. Am. Chem. Soc.* **1967**, *89*, 3712–3720.
56. Faust, B.C.; Hoigne, J. Photolysis of Fe (III)-hydroxy complexes as sources of OH radicals in clouds, fog and rain. *Atmos. Environ. Part A Gen. Top.* **1990**, *24*, 79–89.
57. Sherman, D.M. Electronic structures of iron(III) and manganese(IV) (hydr)oxide minerals: Thermodynamics of photochemical reductive dissolution in aquatic environments. *Geochim. et Cosmochim. Acta.* **2005**, *69*, 3249–3255.
58. Collienne, R.J. Photoreduction of iron in the epilimn ion of acidic lakes. *Limnol. Oceanogr.* **1983**, *28*, 83–100.
59. Mc Knight, D.M.; Kimball, B.A.; Bencala, K.E. Iron photoreduction and oxidation in an acidic mountain stream. *Science* **1988**, *240*, 637–640.
60. Turner, R.C.; Kathleen, E.M. The ultraviolet absorption spectra of the ferric ion and its first hydrolysis product in aqueous solutions. *Can. J. Chem*. **1957**, *35*, 1002–1009.
61. Evans, M.G.; Santappa, M.; Uri, N. Photoinitiated free radical polymerization of vinyl compounds in aqueous solution. *J. Polym. Sci*. **1951**, *7*, 243–260.
62. Feng, W.; Nansheng, D. Photochemistry of hydrolytic iron (III) species and photoinduced degradation of organic compounds. *Chemosphere* **2000**, *41*, 1137–1147.
63. Bates, H.G.; Uri, N. Oxidation of aromatic compounds in aqueous solution by free radicals produced by photo-excited electron transfer in iron complexes. *J. Am. Chem. Soc.* **1953**, *75*, 2754–2759.
64. Mukherjee, A.R.; Ghosh, P.; Chadha, S.C.; Palit, S.R. End group studies in poly (methyl methacrylate) initiated by redox systems containing reducing sulfoxy compounds in aqueous media. *Die Makromol. Chem.* **1966**, 97, 202–208.
65. David, F.; David, P.G. Photoredox chemistry of iron(lll) chloride and iron(lll) perchlorate in aqueous media. A comparative study. *J. Phys. Chem.* **1976**, *80*, 579–583.
66. Nadtochenko, V.A.; Kiwi, J. Photolysis of $FeOH^{2+}$ and $FeCl^{2+}$ in aqueous solution. Photodissociation kinetics and quantum yields. *Inorg. Chem*. **1998**, *37*, 5233–5238.
67. Balzani, V.; Carassiti, V. *Photochemistry of Coordination Compounds*; Academic Press*:* London, UK, 1970.
68. Horvath, O.; Stevenson, K. *Charge-Transfer Photochemistry of Coordination Compounds*; VCH: Weinheim, Germany, 1993.
69. Hasinoff Brian, B. The kinetic activation volumes for the binding of chloride to iron(III), studied by means of a high pressure laser temperatura jump apparatus. *Can. J. Chem*. **1976**, *54*, 1820–1826.
70. Byrne, R.; Kester, D.J. Ultraviolet spectroscopic study of ferric hydroxide complexation. *J. Solut. Chem*. **1978**, *7*, 373–383.

71. Byrne, R.; Kester, D.J. Ultraviolet spectroscopic study of ferric equilibria at high chloride concentrations. *J. Solut. Chem*. **1981**, *10*, 51–67.
72. Polikanin, A.M.; Budkevich, B.A. Photochemical processes in the iron (III) chloride-dye-binder system. *J. Appl. Spectrosc*. **1993**, *59*, 699–704.
73. Oster, G.K.; Oster, G. Photoreduction of metal ions by visible light. *J. Am. Chem. Soc.* **1959**, *81*, 5543–5545.
74. Toshima, N.; Hara, S. Direct synthesis of conducting polymers from simple monomers. *Prog. Polym. Sci*. **1995**, *20*, 155–183.
75. Shirakawa, H.; Louis, E.J.; Diarmid, A.G.; Chiang, A.G.; Heeger, A.J. Synthesis of electrically conducting organic polymers: Halogen derivatives of polyacetylene, (CH)*x*. *J. Chem. Soc. Chem. Commun*. **1977**, *474*, 578–580.
76. Dutta, P.; Biswas, S.; Ghosh, M.; De, S.K.; Chatterjee, S. The DC and AC conductivity of polyaniline–polyalcohol blends. *Synth. Met*. **2000**, *122*, 455–461.
77. Kukhtarev, N.V.; Markov, V.B.; Odulov, S.G.; Soskin, M.S.; Vinetskii, V.L. Holographic storage in electrooptic crystals. *Ferroelectrics* **1978**, *22*, 949–960.
78. De Oliveira, H.P.; dos Santos, M.V.P.; dos Santos, C.G.; de Melo, C.P. Preparation and electrical and dielectric characterization of PVA/PPY blends. *Mater. Charact*. **2003**, *50*, 223–226.

© 2014 by the authors; licensee MDPI, Basel, Switzerland. This article is an open access article distributed under the terms and conditions of the Creative Commons Attribution license (http://creativecommons.org/licenses/by/3.0/).